Zero Echo Time (ZTE) Imaging with Anisotropic Field-of-View

Cheng Li[1], Alan C. Seifert[1], Jeremy F. Magland[1], and Felix W. Wehrli[1]
[1]*Laboratory for Structural NMR Imaging, Department of Radiology, University of Pennsylvania, Philadelphia, PA, United States*

Introduction - Ultrashort echo-time (UTE) (1) and zero echo-time (ZTE) (2,3) imaging techniques are the two most widely used pulse sequences for short-T_2 imaging on clinical MRI scanners. In ZTE imaging the imaging gradient is turned on before RF transmission, which offers a two-fold advantage over UTE imaging. First, the *k*-space is traversed within a shorter time period, resulting in higher SNR and reduced blurring due to less T_2 decay within the data acquisition window. Second, data sampling occurs during the plateau period of the readout gradient, therefore avoiding the image distortion artifact associated with ramp sampling in UTE imaging. However, ZTE is time-intensive for two reasons: 1. ZTE is inherently 3D, which requires a large number of half projections; 2. To fill the missing central *k*-space part due to the dead time of the T/R switch, usually a complementary scan is performed, such as acquiring additional radial projections with lower gradient strength as in WASPI (2), or single point imaging (SPI) as in PETRA (3). In this work, we designed a ZTE sequence with anisotropic filed-of-view (aFOV) tailored to elongated anatomies such as the extremities, as a means to reduce the scan time. To demonstrate the feasibility of aFOV ZTE imaging, point spread function (PSF) simulations, proton phantom imaging and *ex-vivo* cortical bone phosphorus imaging were conducted.

Methods - <u>*Sequence:*</u> The aFOV ZTE imaging sequence is derived from its isotropic counterpart, i.e. PETRA, in which the central *k*-space portion is filled by SPI which entails a Cartesian sampling while the outer portion is sampled with a center-out radial trajectory. SPI for the central part acquisition is preferred since it provides constant effective echo time, resulting in minimal T_2-blurring. However, SPI scanning is relatively slow accounting for a significant portion of total scan time. Depending on the number of missing *k*-space points per half projection, this portion of scan time is substantially reduced in the aFOV ZTE sequence. To generate an asymmetric FOV, the *k*-space sampling patterns of the radial and Cartesian parts are treated separately. The half projections in the 3D radial part are distributed by a spiral-based anisotropic FOV design method (4), while the FOV of the SPI part is controlled by the k-space sampling interval according to $FOV = 1/\Delta k$. To avoid aliasing, the FOV of the SPI portion should be large enough to encompass the whole object. On the other hand, the radial part is allowed to be undersampled due to the diffusive pattern of the streaking artifact. The pulse sequence was implemented on Siemens 3T and 7T scanners with cylindrical and ellipsoid FOV shape.

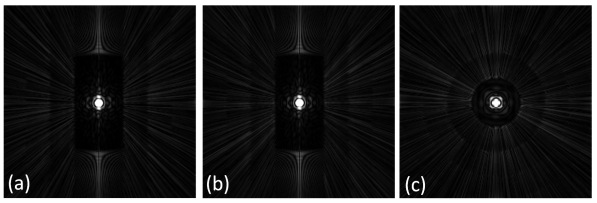

Fig. 1 PSF of ZTE with cylindrical FOV in the (a) x=0, (b) y=0 and (c) z=0 planes

<u>*Image Reconstruction:*</u> The images were reconstructed by solving the following optimization problem: $\hat{m} = \arg\min_m \|Fm - y\|_2^2$ [1]. Here $\hat{m}$ is the reconstructed image, *y* denotes the *k*-space data and *F* represents the non-uniform Fourier transform operator that maps the image onto the *k*-space data according to the sampling trajectory. A linear Conjugate Gradient algorithm was used for solving Eq.1. The Fourier transform operator *F* and its adjoint operator F^H were performed by using the NFFT C library function (5).

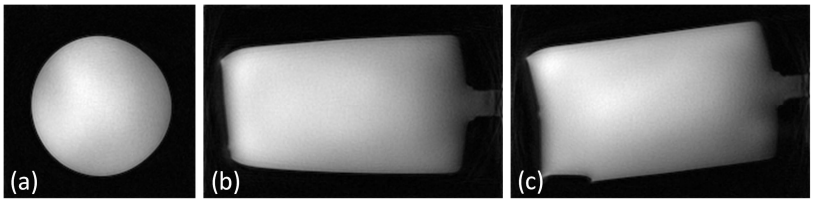

Fig. 2 Water phantom images in the (a) axial, (b) coronal and (c) sagittal views

<u>*Simulation:*</u> PSF simulations were conducted to confirm the desired FOV shape, in which the unit signal is assumed at all the sampled k-space locations. The *k*-space trajectory of the radial portion was designed to generate aliasing-artifact-free FOV of cylindrical shape with diameter of 64 and length of 128. The FOV of the Cartesian portion was 128×128×256 and reconstructed image matrix was 256×256×256.

<u>*Proton Imaging*</u>: A water phantom was imaged at 3T by a ZTE sequence with ellipsoidal FOV using a 4-channel head coil to evaluate image quality. 25870 half-projections were acquired in the radial portion to support artifact-free ellipsoidal FOV with principal axes of 80, 80 mm and 120 mm length. The central *k*-space portion was filled with 1731 single points to support a FOV of 160×160×250 mm^3. TE/TR = 80 μs/10 ms, FA = 5º and 12μs hard pulse duration, readout bandwidth = ±62.5 kHz, reconstructed image matrix = 160×160×250, total scan time = 276 s.

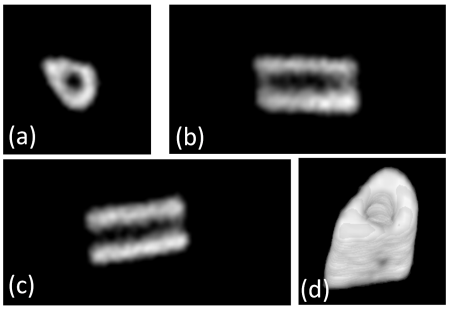

Fig. 3 ^{31}P image slices (a-c) and 3D volume rendering (d)

<u>*Phosphorus Imaging*</u>: A cortical bone specimen of the mid-tibia from an 83 year old female donor was scanned at 7T using a custom-built solenoid RF coil with anisotropic and isotropic FOV ZTE sequences. For the aFOV version, the radial portion consisted of 4872 half projections, resulting in a cylindrical artifact-free FOV of radial part with diameter of 30 mm and length of 60 mm. The SPI portion was acquired in 983 TR cycles and FOV of 160×160×320 mm^3. Other parameters: TE/TR = 50 μs/250 ms, FA=5º, 10μs hard pulse duration, readout bandwidth = ±100 kHz, reconstructed image matrix=128×128×256. For comparison purposes, a PETRA sequence with isotropic FOV of 320×320×320 mm^3 was run with the same protocol except 4139 single points and 5000 half projections supporting a 40 mm isotropic FOV. The scan time of the aFOV ZTE was 24 minutes while its isotropic counterpart took 38 minutes.

Results - Fig. 1 shows the PSF in the (a) *x*=0, (b) *y*=0 and (c) *z*=0 planes, confirming the desired cylindrical FOV shape. The (a) axial, (b) coronal and (c) sagittal views of the water phantom in Fig. 2 show good image quality, except some minor streaking artifact visible at the edge of the images due to undersampling of the radial part. The ^{31}P image slices at different views, along with 3D volume rendition are shown in Fig.3. Excellent image quality is achieved. The blurring in the image is due to the extremely short T_2* of ^{31}P, ~100 μs at 7T. The image SNR is ~20, which is lower than that obtained with the isotropic version (SNR ~30).

Discussion & Conclusions - By tailoring the FOV of ZTE imaging to the shape of the object, the scan time is shortened compared to its isotropic FOV counterpart with comparable image quality, while the image SNR is decreased as expected due to reduced scan time. aFOV ZTE imaging is especially beneficial for non-proton short-T_2 imaging, such as ^{31}P and ^{23}Na imaging, since images are free of contamination from external objects such as polymeric structures of the coil, allowing adjustment of the imaging FOV to the object of interest. A further step to reduce scan time is to incorporate anisotropic resolution, since the signal variation along a particular dimension may be less than other directions in some quantitative imaging applications involving, for example, imaging of the extremities.

References: 1. Gatehouse PD et al. Clin Radiol 2003;58(1):1-19; 2. Wu Y et al. MRM 2003;50(1):59-68; 3. Grodzki DM et al. MRM 2012;67(2):510-8; 4. Larson PEZ et al. IEEE TMI 2008;27(1):47-57; 5. Keiner, J et al. ACM Trans. Math. Software 2009;36(4):19

Acknowledgements: NIH RO1 AR50068, Howard Hughes Medical Institute (HHMI) International Student Research Fellowship.